Action-potential-encoded second-harmonic generation as an ultrafast local probe for nonintrusive membrane diagnostics

M. N. Shneider,[1] A. A. Voronin,[2] and A. M. Zheltikov[2]
[1]*Department of Mechanical and Aerospace Engineering, Princeton University, Princeton, New Jersey 08544-5263, USA*
[2]*Physics Department, International Laser Center, M. V. Lomonosov Moscow State University, Moscow 119992, Russia*
(Received 30 October 2009; revised manuscript received 24 December 2009; published 31 March 2010)

The Hodgkin-Huxley treatment of the dynamics of a nerve impulse on a cell membrane is combined with a phenomenological description of molecular hyperpolarizabilities to develop a closed-form model of an action-potential-sensitive second-harmonic response of membrane-bound chromophores. This model is employed to understand the key properties of the map between the action potential and modulation of the second harmonic from a cell membrane stained with hyperpolarizable chromophore molecules.

DOI: 10.1103/PhysRevE.81.031926 PACS number(s): 87.80.Dj, 42.65.An

I. INTRODUCTION

Nonlinear-optical techniques offer unique options and attractive solutions for optical microscopy and bioimaging. Multiphoton-absorption microscopy has been intensely used through the past two decades for high-resolution deep-tissue imaging of biotissues, including *in vivo* cellular imaging of different organs and various types of tissues, as well as the action potential (AP) in mammalian nerve terminals [1–4]. Microscopy based on second- and third-harmonic generations has been shown to provide valuable information on the texture and morphology of biotissues in three dimensions [5–7]. Coherent anti-Stokes Raman scattering (CARS) and stimulated Raman scattering (SRS) [8,9] enable chemically selective high-resolution, high-speed imaging, suggesting an advantageous approach for the visualization of processes inside living cells [10,11]. Stimulated-emission depletion (STED) and related techniques [12,13] break the records of spatial resolution, offering a unique tool for imaging fine details of biotissues. Recent advances in fiber technologies [14,15] allow bulky free-space components to be replaced by appropriate fiber-format elements and devices, making nonlinear-optical imaging systems flexible, robust, and fully compatible with requirements of *in vivo* work and real-life applications.

Extension of advanced concepts of nonlinear-optical imaging to neuroscience is one of the most challenging and interesting tasks in biophotonics. In a pioneering experiment published more than four decades ago, Cohen *et al.* [16] have demonstrated the possibility of nerve activity visualization through the detection of light-induced birefringence of nonmyelinated nerve fibers. In more recent work [17–25], second-harmonic generation (SHG) and two-photon excitation of voltage-sensitive dyes [4] have been shown to offer powerful tools for the sensing of action potentials on a membrane. A linear dependence of the SHG signal from membrane-bound chromophore molecules on the membrane potential with a sign reversal at zero voltage has been demonstrated by Nuriya *et al.* [24]. Evans *et al.* [26] employed CARS microscopy for *in vitro* imaging of brain structure. Specifically designed fiber components have been shown to enable fiber-format detection of neuron activity in brain of transgenic mice using the luminescence response of two-photon-excited fluorescent-protein neuron-activity reporters [27,28].

Here, we propose a closed-form model of AP-induced SHG modulation on a cell membrane labeled with hyperpolarizable molecules. This model combines the Hodgkin-Huxley treatment of the dynamics of a nerve impulse with a phenomenological description of the second-harmonic response in terms of molecular hyperpolarizabilities. We will apply this model to understand the key properties of the map between the AP and modulation of the second-harmonic response of a membrane-bound chromophore.

II. ACTION POTENTIAL ON A SPATIALLY NONUNIFORM NEURON MEMBRANE

We start our analysis of action potentials on a neuron membrane with the well-known Hodgkin-Huxley model [29–31], which represents a lipid bilayer of a cell membrane as a capacitance c_m [Fig. 1(a)], with potassium and sodium ion channels included through the conductances G_K and G_{Na}, respectively, and the leakage of all the other ions included through the conductance G_L. The batteries V_K, V_{Na}, and V_L in Fig. 1(a) mimic the electrochemical gradients, controlling the flows of potassium, sodium, and all the other ions. The resulting equation for the voltage V_m across the membrane is written as

$$\frac{1}{rc_m}\frac{\partial^2 V_m}{\partial x^2} - \frac{\partial V_m}{\partial t} = \frac{j_i}{C}. \tag{1}$$

Here, x is the coordinate along the membrane, t is the time, r is the membrane resistance per unit length, C is the membrane capacity per unit area, and j_i is the total ion current density through the membrane,

$$j_i = G_{Na}m^3h(V_m - V_{Na}) + G_K n^4(V_m - V_K) + G_L(V_m - V_L), \tag{2}$$

where m, h, and n are the sodium activation, sodium inactivation, and potassium activation control parameters, which vary within an interval from 0 to 1 and are governed by the following set of first-order differential equations:

$$\frac{dn}{dt} = \alpha_n(1-n) - \beta_n n, \tag{3}$$

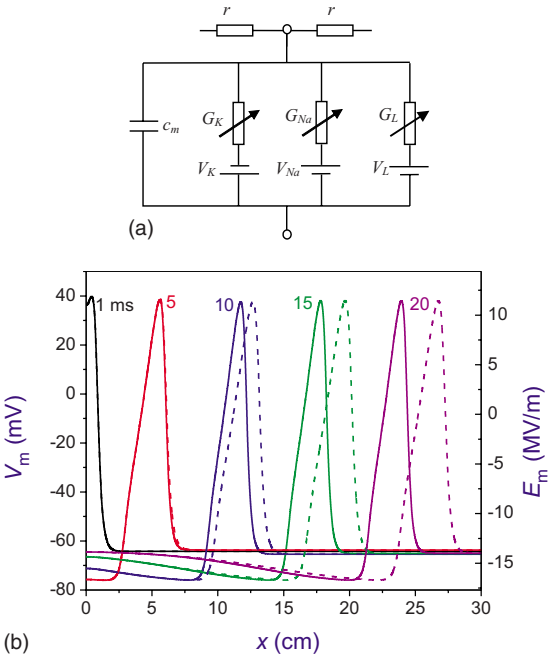

FIG. 1. (Color online) (a) An electric-circuit diagram of the Hodgkin-Huxley-type model of a cell membrane. (b) An action potential propagating along a nonmyelinated axon with $c_m=1.5\times10^{-7}$ F/cm, $C=10^{-6}$ F/cm^2, $a=238$ μm, $G_K=0.036$ Ω^{-1} cm^{-2}, $G_{Na}=0.12$ Ω^{-1} cm^{-2}, $G_L=3\times10^{-4}$ Ω^{-1} cm^{-2}, $V_K=-77$ mV, $V_{Na}=50$ mV, $V_L=-54.4$ mV, $V_R=-65$ mV, and $\delta_m\approx4.5$ nm, with $r=2.0\times10^4$ Ω/cm (solid line), and r changing in a stepwise fashion from 2.0×10^4 to 1.5×10^4 Ω/cm at $x=6$ cm (dashed line) at different instants of time (1, 5, 10, 15, and 20 ms), as indicated in the figure.

$$\frac{dm}{dt} = \alpha_m(1-m) - \beta_m m, \tag{4}$$

$$\frac{dh}{dt} = \alpha_h(1-h) - \beta_h h. \tag{5}$$

The coefficients α_j and β_j $(j=n,m,h)$ in Eqs. (3)–(5) are given by empirical relations, which, at the temperature $T=6.3$ °C, take the form $\alpha_n=(0.1-0.01u)/[\exp(1-0.1u)-1]$, $\alpha_m=(2.5-0.1u)/[\exp(2.5-0.1u)-1]$, $\alpha_h=0.07\exp(-u/20)$, $\beta_n=0.125\exp(-u/80)$, $\beta_m=4\exp(-u/18)$, and $\beta_h=[\exp(3-0.1u)+1]^{-1}$, where $u\equiv u(x,t)=V_m(x,t)-V_R$, V_R is the resting potential, and all the potentials are measured in millivolts. For higher temperatures, $T\geq6.3$ °C, these coefficients are calculated by multiplying the values of α_j and β_j defined by expressions above by a factor $k=3^{[(T-6.3)/10]}$.

Calculations were performed at the temperature $T=6.3$ °C for typical parameters of a giant squid axon [30,31]: $c_m=1.5\times10^{-7}$ F/cm and $C=c_m/2\pi a=10^{-6}$ F/cm^2, where $a=238$ μm is the axon radius, $G_K=0.036$ Ω^{-1} cm^{-2}, $G_{Na}=0.12$ Ω^{-1} cm^{-2}, $G_L=3\times10^{-4}$ Ω^{-1} cm^{-2}, $V_K=-77$ mV, $V_{Na}=50$ mV, $V_L=-54.4$ mV, and $V_R=-65$ mV. The electric field across a membrane can be calculated from the solution to Eq. (1) as $E_m(x,t)=V_m(x,t)/\delta_m$, where δ_m is the membrane thickness (here, $\delta_m\approx4.5$ nm).

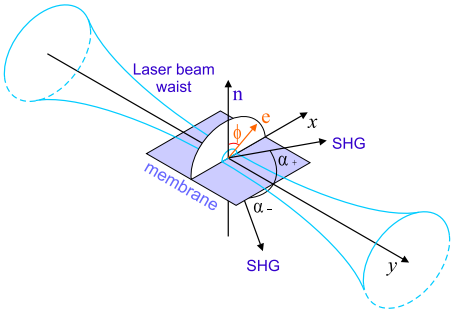

FIG. 2. (Color online) Probing the membrane potential with second-harmonic generation: **n** is the normal to the membrane surface, **e** is the polarization of the pump field, α_+ and α_- are the second-harmonic emission angles.

In Fig. 1(b), we plot the membrane potential and the electric field calculated by solving Eq. (1) for a membrane with a constant resistance, $r=2.0\times10^4$ Ω/cm (solid line) and a membrane with a resistance changing in a stepwise fashion from 2.0×10^4 to 1.5×10^4 Ω/cm at $x=6$ cm (dashed line). Such a variation in r models changes in membrane permeability can be induced by various damage mechanisms, including electroporation [31]. In calculations with a varying r, we assume for simplicity that all the other membrane parameters defining the action potential in the Hodgkin-Huxley model remain unchanged. As can be seen in Fig. 1, reduction of r increases the AP speed, giving rise to a detectable advancement of the AP at a given x relative to the AP propagating on a membrane with constant r. At $t=20$ ms, as can be also seen from Fig. 1, the separation between the APs is as large as 3.5 cm. In the following section, we will demonstrate that, due to the high amplitude of the electric field generated across the axon membrane [$E_m\approx7-8$ MV/m in Fig. 1(b)] this change in the AP speed can be readily detected through the change in SHG from a membrane covered by push-pull chromophores.

III. MEMBRANE DIAGNOSTICS WITH SECOND-HARMONIC GENERATION

We now assume that the membrane is labeled with hyperpolarizable dye molecules, which generate the second-harmonic in response to the incident laser field. This technique for membrane potential imaging has been earlier successfully demonstrated with various types of amphiphilic push-pull chromophore dyes [18–25]. For an incident laser beam polarized along the normal to the membrane surface (Fig. 2), the intensity of the second harmonic generated by hyperpolarizable dye molecules in the presence of an action potential is given by [18–20]

$$I(E_m) = I_0[1+\kappa E_m(1-\theta)], \tag{6}$$

where $I_0=I(E_m=0)$ is the second-harmonic intensity in the absence of the membrane potential, $\theta=\langle\sin^2\delta\cos\delta\rangle(2\langle\cos^3\delta\rangle)^{-1}$ is the order parameter, δ being the tilt angle of molecules aligned by the laser field from the normal to the membrane surface, and $\kappa=2\,\mathrm{Re}(\gamma/\beta)$, with $\beta\equiv\beta(2\omega;\omega,\omega)$ and $\gamma\equiv\gamma(2\omega;\omega,\omega,0)$ being the first- and

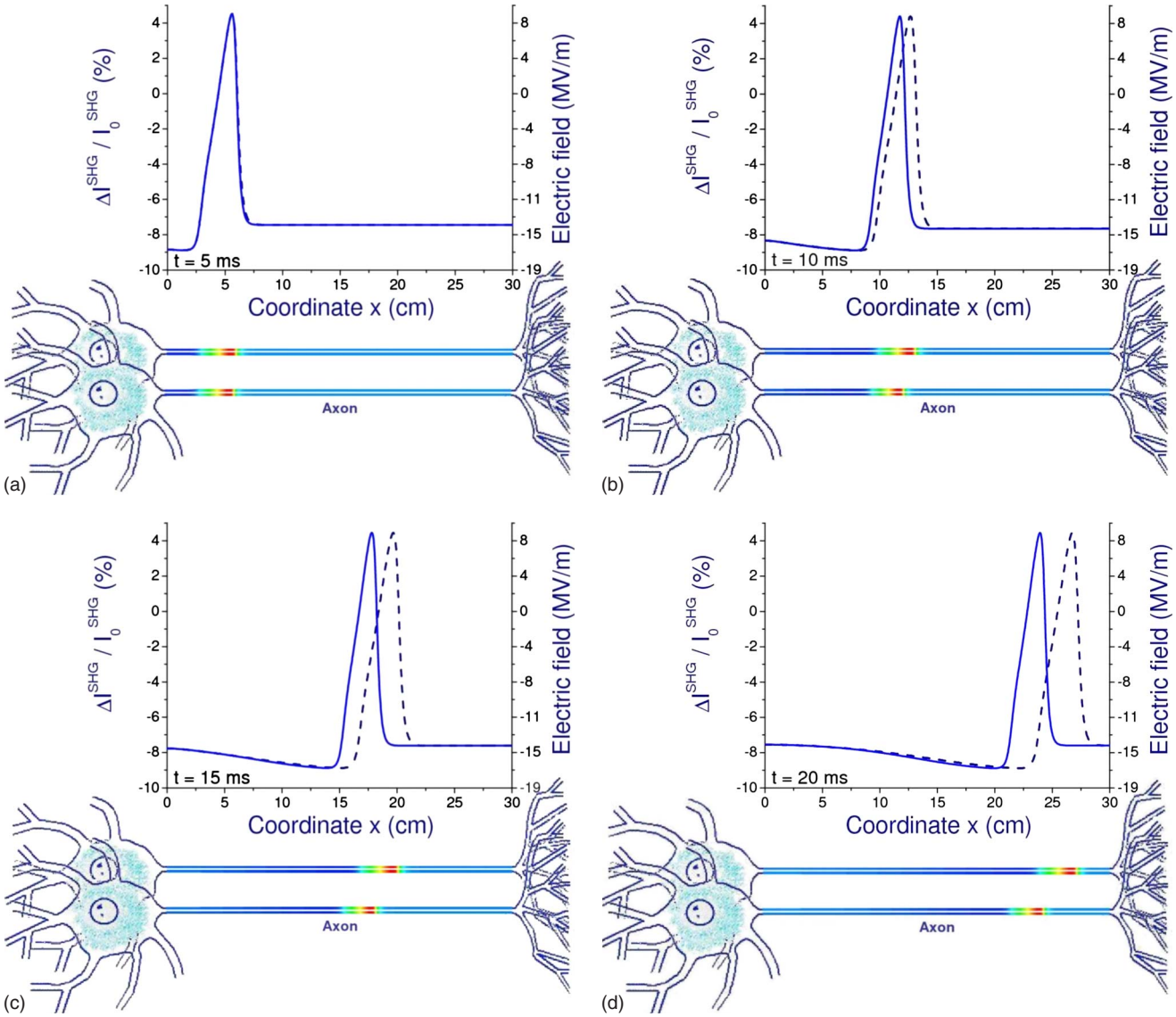

FIG. 3. (Color online) Snapshots of the differential second-harmonic signal $\Delta I/I_0=(I-I_0)/I_0$ for a membrane with $r=2.0\times10^4$ Ω/cm (solid lines) and r changing in a stepwise fashion from 2.0×10^4 to 1.5×10^4 Ω/cm at $x=6$ cm (dashed lines) sampled with ultrashort laser pulses at different instants of time: (a) 5, (b) 10, (c) 15, and (d) 20 ms. The electric field in the action potential is shown on the right axis. Parameters of calculations are specified in the text. Images of the AP-modulated differential second-harmonic signal for a membrane with a constant and varying r are shown in the lower part of each panel.

second-order hyperpolarizabilities of molecular labels.

As can be seen from Eq. (6), SHG provides a linear map between the action potential and modulation of the second harmonic. To quantify the sensitivity of the second-harmonic signal to the membrane potential, we use the following approximate expressions for the hyperpolarizabilities β and γ [18–20]:

$$\beta \approx 2|\mu_{eg}|^2 \Delta\mu D(\omega), \tag{7}$$

and

$$\gamma \approx 2|\mu_{eg}|^2 D(\omega)\left[\frac{\Delta\mu^2}{\hbar(\omega_{eg}-2\omega-i\Gamma)}-\frac{4(\Delta\mu^2-|\mu_{eg}|^2)}{\hbar(\omega_{eg}-i\Gamma)}\right], \tag{8}$$

where ω is the pump frequency, $D(\omega)=[\hbar^2(\omega_{eg}-2\omega-i\Gamma)(\omega_{eg}-\omega-i\Gamma)]^{-1}$, ω_{eg} and μ_{eg} are the frequency and the dipole moment of the transition between the ground and excited states involved in SHG, Γ is the decay constant, and $\Delta\mu$ is the difference of dipole moments in the excited and ground states.

We now apply Eqs. (1)–(8) to analyze the AP-induced modulation of SHG on a cell membrane with FM4-64 intracellular SHG chromophore, which has been successfully used [22–25] to image the membrane potential in neurons.

Parameters of this chromphore were determined from the change in the SHG response to a 100 mV depolarization measured by Yuste's group [25] for different laser wavelengths ($10.3 \pm 0.8\%$ at 850 nm, $10.6 \pm 1.1\%$ at 900 nm, and $14.8 \pm 1.2\%$ at 1064 nm). Applying Eqs. (6)–(8) to fit these data with $\delta \approx 36°$ (which was the case in Ref. [24]), we find $\lambda_{eg} = 2\pi c/\omega_{eg} \approx 560 \pm 20$ nm, $\Gamma \approx (0.33 \pm 0.03)\omega_{eg}$, $\mu_{eg} \approx 10 \pm 10$ D, $\Delta\mu \approx 150 \pm 10$ D, $\theta \approx 0.26$, $|\beta| \approx 3.8 \times 10^{-47}$ C m^2 V^{-2}, and $k \approx 7 \times 10^{-9}$ m/V for a pump wavelength of 800 nm. The number of photons emitted in the second harmonic can be estimated as $N_{SH} \approx N^2 \sigma_{SHG} I_p^2/2$, where N is the number of molecules in the interaction region, I_p is the pump intensity, and $\sigma_{SHG} = 4n_{2\omega}\hbar\omega^5|\beta|^2(3\pi)^{-1}n_\omega^{-2}\varepsilon_0^{-3}c^{-5}$ is the SHG cross section with n_ω and $n_{2\omega}$ being the refractive indices at pump and second-harmonic frequencies. For dye molecules with the above-specified parameters, the SHG cross section is estimated as $\sigma_{SHG} \approx 0.021$ GM for a pump wavelength of 800 nm.

The number of molecules on the surface of a membrane contributing to SHG is given by $N = \rho_s S$, where ρ_s is the surface density of hyperpolarizable dye molecules and S is the area of the pump-irradiated region on a membrane surface. With a typical surface density of hyperpolarizable dye molecules $\rho_s \approx 10^{12}$ cm^{-2} [18] and the laser-irradiated area S estimated as $S \approx 2ad_p \approx 100$ μm^2 for an axon radius $a \approx 0.5$ μm (a typical radius of nonmyelinated axons in human body) and a diameter of the focused pump beam $d_p \approx 100$ μm, molecules with $\sigma_{SHG} \approx 0.021$ GM excited with a pump pulse with a pulse width $\tau_p \approx 100$ fs and the beam area $d_p^2 \approx 10^{-4}$ cm^2 will generate approximately 175 second-harmonic photons per each 100 fs pump pulse with an energy of 10 nJ, yielding a readily detectable signal at high pump pulse repetition rates. Even more intense second-harmonic signals can be expected for a squid giant axon, where the laser-irradiated area for the above-specified pump parameters is much larger, $S \approx d_p^2 \approx 10^{-4}$ cm^2, leading to an estimate of 2×10^6 for the number of second-harmonic photons per 100 fs, 10 nJ pump pulse.

The snapshots of the differential second-harmonic signal $\Delta I/I_0 = (I - I_0)/I_0$, measured by sampling the membrane potential with ultrashort laser pulses are presented in Figs. 3(a)–3(d). With a typical speed of the AP in nonmyelinated axons estimated as 10–20 m/s and a typical spatial extension of the positive-polarity section of the AP $L_{AP} \approx 3$ cm [Figs. 1(b) and 3(a)–3(d)], the time duration of the positive-polarity part of the AP is $\tau_{AP} \approx 1.5$ ms. Laser pulses with $\tau_p \approx 100$ fs and $d_p \approx 100$ μm thus serve as an almost ideal sampler for such a wave process providing spatial and temporal uncertainties as low as $d_p/L_{AP} \approx 3 \times 10^{-3}$ and $\tau_p/\tau_{AP} \approx 6 \times 10^{-11}$. With a typical time required to take a single frame of the SHG profile on a membrane-bound chromophores estimated as $\tau_f \approx 10$ μs [23], the AP dynamics can be captured in such frames with a time resolution of $t/\tau_{AP} \approx 6 \times 10^{-3}$.

The Hodgkin-Huxley model-based analysis of membrane potentials is, rigorously speaking, applicable only to nonmyelinated nerve fibers. The proposed SHG-based membrane potential metrology technique can, however, be extended to myelinated fibers. While the speed of action potentials in nonmyelinated fibers scales as $a^{1/2}$ with the axon radius a, myelinated fibers support nerve impulses with a speed $\propto a$. As a result, when the myelin sheath is damaged or destroyed, the AP speed drastically decreases [32–36]. This change in the AP speed can be readily detected by the SHG technique as described above.

IV. CONCLUSION

The Hodgkin-Huxley treatment of the dynamics of a nerve impulse on a cell membrane has been combined in this work with a phenomenological description of molecular hyperpolarizabilities to develop a closed-form model of an AP-sensitive second-harmonic response of membrane-bound chromophores. This model was employed to understand the key properties of the map between the action potential and modulation of the second harmonic from a cell membrane stained with hyperpolarizable chromophore molecules. Our analysis shows, in particular, that AP-sensitive SHG by membrane-bound chromophores suggests an attractive technique for nonintrusive detection and high-resolution imaging of spatial inhomogeneities and defects on nerve fibers.

ACKNOWLEDGMENTS

We are grateful to K. V. Anokhin and L. Shinkarenko (Lurya) for stimulating discussions and encouragement. This work was supported in part by the Federal Program of the Russian Ministry of Education and Science (Contracts No. 1130 and No. 02.740.11.0223). Research by A.A.V. was also partially supported by the Russian Foundation for Basic Research Projects No. 08-02-92226, No. 08-02-92009, No. 09-02-12359, and No. 09-02-92119.

[1] W. Denk, J. H. Strickler, and W. W. Webb, Science **248**, 73 (1990).
[2] W. R. Zipfel, R. M. Williams, and W. W. Webb, Nat. Biotechnol. **21**, 1369 (2003).
[3] F. Helmchen and W. Denk, Nat. Methods **2**, 932 (2005).
[4] J. A. N. Fisher, J. R. Barchi, C. G. Welle, G.-H. Kim, P. Kosterin, A. Lía Obaid, A. G. Yodh, D. Contreras, and B. M. Salzberg, J. Neurophysiol. **99**, 1545 (2008).
[5] P. J. Campagnola, H. A. Clark, W. A. Mohler, A. Lewis, and L. M. Loew, Nat. Biotechnol. **21**, 1356 (2003).
[6] D. Yelin and Y. Silberberg, Opt. Express **5**, 169 (1999).
[7] A. A. Ivanov, M. V. Alfimov, and A. M. Zheltikov, Phys. Usp. **47**, 687 (2004).
[8] G. L. Eesley, *Coherent Raman Spectroscopy* (Pergamon, Oxford, 1981).
[9] A. M. Zheltikov and N. I. Koroteev, Phys. Usp. **42**, 321 (1999).
[10] J.-X. Cheng and X. S. Xie, J. Phys. Chem. B **108**, 827 (2004).

[11] C. W. Freudiger, W. Min, B. G. Saar, S. Lu, G. R. Holtom, C. He, J. C. Tsai, J. X. Kang, and X. Sunney Xie, Science **322**, 1857 (2008).
[12] S. W. Hell, Nat. Biotechnol. **21**, 1347 (2003).
[13] S. W. Hell, Nat. Methods **6**, 24 (2009).
[14] P. St. J. Russell, J. Lightwave Technol. **24**, 4729 (2006).
[15] A. M. Zheltikov, Phys. Usp. **50**, 705 (2007).
[16] L. B. Cohen, R. D. Keynes, and B. Hille, Nature (London) **218**, 438 (1968).
[17] O. Bouevitch, A. Lewis, I. Pinevsky, J. P. Wuskell, and L. M. Loew, Biophys. J. **65**, 672 (1993).
[18] L. Moreaux, O. Sandre, M. Blanchard-Desce, and J. Mertz, Opt. Lett. **25**, 320 (2000).
[19] L. Moreaux, O. Sandre, and J. Mertz, J. Opt. Soc. Am. B **17**, 1685 (2000).
[20] L. Moreaux, T. Pons, V. Dambrin, M. Blanchard-Desce, and J. Mertz, Opt. Lett. **28**, 625 (2003).
[21] T. Pons, L. Moreaux, O. Mongin, M. Blanchard-Desce, and J. Mertz, J. Biomed. Opt. **8**, 428 (2003).
[22] B. A. Nemet, V. Nikolenko, and R. Yuste, J. Biomed. Opt. **9**, 873 (2004).
[23] D. A. Dombeck, L. Sacconi, M. Blanchard-Desce, and W. W. Webb, J. Neurophysiol. **94**, 3628 (2005).
[24] M. Nuriya, J. Jiang, B. Nemet, K. B. Eisenthal, and R. Yuste, Proc. Natl. Acad. Sci. U.S.A. **103**, 786 (2006).
[25] J. Jiang, K. B. Eisenthal, and R. Yuste, Biophys. J. **93**, L26 (2007).
[26] C. L. Evans, X. Xu, S. Kesari, X. Sunney Xie, S. T. C. Wong, and G. S. Young, Opt. Express **15**, 12076 (2007).
[27] L. V. Doronina, I. V. Fedotov, O. I. Ivashkina, M. A. Zots, K. V. Anokhin, Yu. M. Mikhailova, A. A. Lanin, A. B. Fedotov, M. N. Shneider, R. B. Miles, A. V. Sokolov, M. O. Scully, and A. M. Zheltikov, Proceedings of the 18th International Laser Physics Workshop, Barcelona, 2009, p. 58.
[28] L. V. Doronina, I. V. Fedotov, A. A. Voronin, O. I. Ivashkina, M. A. Zots, K. V. Anokhin, E. Rostova, A. B. Fedotov, and A. M. Zheltikov, Opt. Lett. **34**, 3373 (2009).
[29] A. L. Hodgkin and A. F. Huxley, J. Physiol. **117**, 500 (1952).
[30] A. Scott, *Neuroscience: A Mathematical Primer* (Springer, New York, 2002).
[31] J. Malmivuo and R. Plonsey, *Bioelectromagnetism: Principles and Applications of Bioelectric and Biomagnetic Fields* (Oxford University Press, New York, 1995).
[32] *Electromagnetics in Biology*, edited by M. Kato (Springer, Tokyo, 2006).
[33] I. Tasaki and K. Frank, Am. J. Physiol. **182**, 572 (1955).
[34] W. I. McDonald, Brain **86**, 481 (1963).
[35] Z. J. Koles and M. Rasminsky, J. Physiol. **227**, 351 (1972).
[36] F. N. Quandt and F. A. Davis, Biol. Cybern. **67**, 545 (1992).